Quaternary Research 79 (2013) 452–457

Contents lists available at SciVerse ScienceDirect

Quaternary Research

journal homepage: www.elsevier.com/locate/yqres

Soil–landscape response to mid and late Quaternary climate fluctuations based on numerical simulations

Sagy Cohen [a,b,c,*], Garry Willgoose [a], Greg Hancock [b]

[a] School of Engineering, The University of Newcastle, Callaghan, New South Wales 2308, Australia
[b] School of Environmental and Life Sciences, The University of Newcastle, Callaghan, New South Wales 2308, Australia
[c] Department of Geography, University of Alabama, Box 870322, Tuscaloosa, AL 35487, USA

ARTICLE INFO

Article history:
Received 8 June 2012
Available online 13 February 2013

Keywords:
Soil Landscape Evolution
Modeling
Pedogenesis
Climate
Middle Quaternary
Late Quaternary
Sediment Transport
Physical Weathering

ABSTRACT

We use a numerical dynamic soil–landscape model to study one aspect of the spatio-temporal soil–landscape evolution process, the effect of climatic fluctuations on soil grading distribution in space and time in response to the interplay between physical weathering and surface erosion (soil mineralogical fluxes). We simulate a synthetic soil–landscape system over the middle and late Quaternary (last 400 ka). The results show that (1) soil–landscape response to climate change is non-linear and highly spatially variable, even at hillslope scale; and (2) soil–landscape adjustment to climate change can lag tens of thousands of years and is both spatially and temporally variable. We propose that the legacy of past climatic condition (i.e. last glacial maximum) in modern soil–landscape systems vary considerably in space. This implies that the spatiotemporal uniformity in which soil is typically described in Earth system modeling and analysis (e.g. carbon cycle) grossly underestimates their actual complexity.

© 2013 University of Washington. Published by Elsevier Inc. All rights reserved.

Introduction

Environmental systems are complex and respond non-linearly to extrinsic and intrinsic forcing. Autogenic feedbacks add a layer of complexity that makes understanding the role of environmental variables difficult. This is particularly true for soil systems due to the multi-dimensionality and long response time of many soil–landscape evolution processes (Jenny, 1941; Sommer et al., 2008; Cornu et al., 2009; Dosseto et al., 2010). Most processes in the terrestrial, aquatic and atmospheric systems are affected by soil–landscape properties (e.g. carbon cycle (Cox et al., 2000), biogeochemical-vegetation interactions (Pan et al., 1996; Sitch et al., 2003; Holmes et al., 2004; Quinton et al., 2010), vegetation root zone extent (Schenk and Jackson, 2002) and sedimentary basin dynamics (Zhang et al., 2001)). Climate is one of the most important factors in soil formation (Birkeland, 1974; Murphy, 2007). Elucidating the effect of climate on soil–landscape evolution is therefore warranted.

The impact of paleoclimate on soils has been studied mainly in the biogeochemical aspects of soil development (Gibbs and Kump, 1994; Chadwick et al., 1995; White and Blum, 1995; West et al., 2005; Zembo et al., 2012). Moreover, the complexity of the soil-climate relationships and the difficulties in separating the individual effects of past processes in existing observations has resulted in mostly qualitative and pedon-scale understandings of soil-paleoclimate relationships (Sommer et al., 2008). This study provides, to the best of our knowledge, the first quantitative and spatially explicit investigation of the effect of climate oscillation on soil–landscape evolution. Our governing hypothesis is that soil–landscape response to climate fluctuations varies non-linearly in space due to heterogeneity in the effect of climate change on the dynamics between soil production and removal (weathering and erosion respectively). Based on our previous studies (Cohen et al., 2009, 2010) we further hypothesize that sharp Quaternary climate changes (e.g. the transition from the last glacier maximum (LGM) to Holocene climate) was faster than the soil–landscape adjustment rate resulting in a prolonged legacy of past climate (e.g. LGM) on modern soil–landscape systems.

Climate control on soil processes includes two main factors, temperature and precipitation. Temperature influences the rate of chemical reactions and biological processes in soil (Birkeland, 1974) as well as freeze-thaw mechanical weathering. Precipitation influences soil erosion rate and the soil water cycle. This soil-water cycle is also a major factor in chemical weathering, leaching and biotic activity (not included in this study). In general it is recognized that hotter and wetter climates are associated with thick and well-developed soils (i.e. high soil production rates) whereas a reduction in one or both factors slows soil production (Murphy, 2007). The spatial transfer of sediments through the process of erosion and deposition has a major effect on lateral and vertical soil distribution (Murphy, 2007). The link between paleoclimate and sediment transfer rates has been recorded mainly in the context of erosion rates and landform

* Corresponding author at: Department of Geography, University of Alabama, Box 870322, Tuscaloosa, AL 35487, USA. Fax: +1 205 348 2278.
E-mail address: sagy.cohen@as.ua.edu (S. Cohen).

0033-5894/$ – see front matter © 2013 University of Washington. Published by Elsevier Inc. All rights reserved.
http://dx.doi.org/10.1016/j.yqres.2013.01.001

https://doi.org/10.1016/j.yqres.2013.01.001 Published online by Cambridge University Press

evolution at varying time scales (e.g. Leeder et al., 1998; Heimsath et al., 2001; Temme and Veldkamp, 2009). However, the effect of paleoclimate fluctuations on the long-term redistribution of soil has been largely ignored mostly due to a lack of spatially distributed data and the complexity of the processes involved.

In this paper we study one aspect of the soil-climate dynamics, the effect of climatic oscillation on soil–landscape evolution. More specifically we investigate the evolution of surface soil grading as a function of the interplay between physical weathering and surface erosion (soil mineralogical fluxes), both driven by climate fluctuations and hillslope topography. The soil–landscape evolution in this study is the sum of the interactions between the weathering process, which generates finer particles, and the erosion process which selectively removes the finer particles. Under stable conditions the model will reach an equilibrium soil grading that varies in space (Cohen et al., 2009, 2010). The spatial distribution of this equilibrium soil grading and the time it takes to reach it is a function of the interplay between weathering and erosion rates (Sharmeen and Willgoose, 2006; Cohen et al., 2010). Our main goal here is to use this narrow set of parameters as a simplified descriptor of this complex system thus promoting conceptual understandings to be fostered in future, increasingly complex, analyses.

Methods

The model

We use a dynamical soil–landscape evolution model (mARM3D; Cohen et al., 2009, 2010) to simulate the soil–landscape physics as a state-space system. mARM3D is a modular and computationally efficient modeling platform allowing explicit, three-dimensional, description of the soil–landscape physics in both space and time. Below we provide a short description of the theoretical background and relevant governing equations. For full description of the model architecture please refer to Cohen et al. (2009, 2010).

For each pixel on the landscape a soil profile is modeled with a user-defined number of layers where the top layer is the surface layer exposed directly to size-selective erosion (Fig. 1b). Erosion rate (E) from the surface layer is calculated as

$$E = e\frac{Q^{c_1}S^{c_2}}{d_{50s}^{c_3}} \tag{1}$$

where e is an empirical erosivity factor (unitless), Q is discharge per unit width ($m^3/s/m$; assumed to increase linearly with contributing area), S is topographic slope, d_{50s} is the median diameter (units m) of the material in the surface layer, and c_1, c_2 and c_3 are calibration parameters (here $c_1 = 1$, $c_2 = 1.2$, $c_3 = 1$ and $e = 0.025$; the model calibration is discussed at Cohen et al., 2009).

The selective entrainment of fine material from the surface is

$$A_{kk} = \begin{cases} \dfrac{a}{d_k^m}g_k & for \quad k < M \\ b\dfrac{a}{d_k^m}g_k & for \quad k = M \\ 0 & for \quad k > M \end{cases} \tag{2}$$

where A is the erosion transition matrix which defines the relative portion of each grading size-class k ($k = 1$ is the smallest-diameter grading class) in the eroded sediment flux, g_k is the soil grading size-class vector (in %), d_k is the mean diameter (units m) of size class k, the power m needs to be calibrated (here $m = 4$), a and b are scaling factors, and M is a size threshold that determines the largest particle diameter that can be entrained in the flow as determined by Shield's shear-stress threshold. Transitions metrics and vectors are used in mARM3D because they are a convenient and computationally efficient mathematical expression of change in soil grading as loss (or enrichment) in one size class necessarily means enrichment (or loss) in all other size classes. The sediment diameter dependency in Eq. (2) is such that for $m > 1$ the erosion process preferentially removes the finer material from the surface, resulting eventually, in the absence of other processes, in a surface armor of coarse particles.

Underlying the surface layer are profile layers subject to bedrock and soil weathering (soil weathering is also simulated for the surface layer). Here we only consider physical weathering calculated by breaking a parent particle into two daughter particles. As mass conservation is assumed the diameters of the daughter particles (d_1, d_2) can be determined from the diameter of the parent particle (d_0):

$$d_1 = \frac{d_0}{(1+n^3)^{1/3}}; d_2 = \frac{d_0}{(1+(1-n)^3)^{1/3}} \tag{3}$$

where n is the geometry of the particle breakdown. Based on experimental studies presented by Wells et al. (2008) we used a split-in-half geometry where $n = 0.5$ which leads to $d_1 = d_2$.

A bedrock and soil weathering depth-dependency equation is used to set the weathering rate in each profile layer as a function of its depth relative to the surface (Heimsath et al., 1997). A modified version of the 'Humped' soil-production function proposed by Minasny and McBratney (2006) is modeled

$$W_l = P_0[\exp(-\delta_1 h_l + P_a) - \exp(-\delta_2 h_l)] \tag{4}$$

where W is the physical weathering rate for profile layer l, P_0 and P_a (mm/yr) are the potential (or maximum) and steady-state weathering rates respectively, h (m) is the thickness of soil above layer l and δ_1 and δ_2 are constants. The values proposed by Minasny and McBratney (2006) of $P_0 = 0.25$ mm/yr, $\delta_1 = 4$, $\delta_2 = 6$, $P_a = 0.005$ mm/yr are used here. Temporal changes in weathering rate are expressed by variability in P_0.

Underlying the profile layers is a semi-infinite bedrock layer, which is considered an infinite source of bedrock to the layer directly above it (Fig. 1b). Soil grading evolves as bedrock and soil particles break into smaller soil particles through weathering and by selective

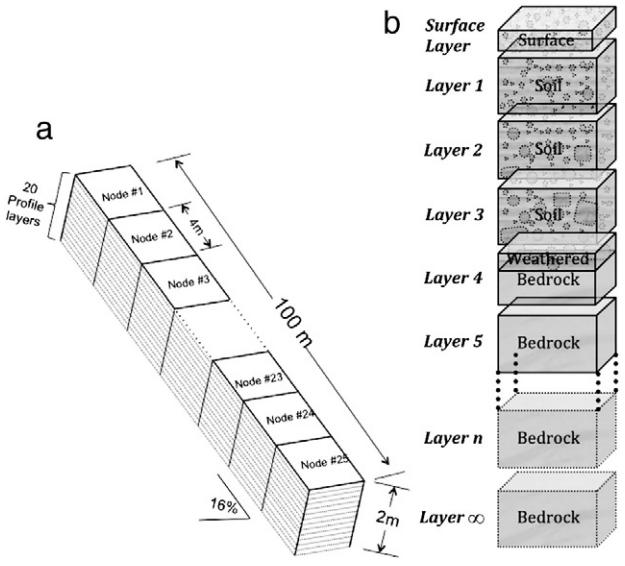


Figure 1. a: synthetic one-dimensional hillslope used in simulations, 100 m long divided into 25 equally spaced nodes each with 20 profile layers, planar shaped at 16% slope. b: illustration of the soil-profile layers in a single node on the hillslope. At the start of the simulation all layers (each 10 cm thick), except for the thin surface layer (0.5 cm thick), contain only bedrock. During the simulation soil is produced from bedrock by weathering. Weathering rate is a function of the depth. Soil particles are removed from the surface layer by erosion, and fine particles are selectively entrained.

https://doi.org/10.1016/j.yqres.2013.01.001 Published online by Cambridge University Press

removal of small, entrainable, particle sizes from the surface layer through erosion by overland flow. When erosion occurs soil is redistributed between adjacent profile layers at a quantity proportional to the surface erosion rate. In Fig. 1b, for example, soil removed from the surface layer by overland flow will be resupplied from Layer 1. The same amount of material will be resupplied from Layer 2 to Layer 1 and so on down the profile.

The parameters were calibrated (Sharmeen and Willgoose, 2006; Wells et al., 2006) for a hydrothermally altered schist from northern Australia subject to a tropical monsoonal climate (average rainfall ~1100 mm/yr) where the authors have worked extensively for the past two decades. The physical weathering rate of the rock (at least for rock particle sizes larger than the mineral crystal size) is higher than other igneous and metamorphic rocks from the region due to its hydrothermal alteration and our results will reflect this higher weathering rate. Though calibrated with site-specific data at our disposal the simulation discussed here are conceptual and do not attempt to realistically simulate a specific site or region.

The climate driver

In this conceptual study we assume a 50% reduction in weathering rate during the LGM (Fig. 2) based on the van't Hoff temperature law of a factor of two to three increase in chemical reaction velocity for every 10^0C rise in temperature. Even though we do not directly simulate chemical weathering in this study, we use it as a proxy to the overall weathering-rate change as a function of temperature. We also assume a 50% reduction in runoff discharge during the LGM loosely based on Coventry (1976) who suggested that mean annual precipitation during the LGM was about half its current level in eastern Australia. These two assumptions are also supported by Gislason et al. (2009) who found in Iceland that a 1^0C increase in temperature resulted in a 4–14% increase in chemical weathering, 8–30% increase in mechanical weathering and 6–16% increase in runoff.

The impact of climate change is modelled as a 5% linear decrease in weathering rate and runoff discharge for every 1°C cooling in temperature (Fig. 2). The Vostok Antarctic research station ice-core time series is employed as a climate forcing (Petit et al., 1999; Fig. 2) by adjusting the discharge parameter Q in Eq. (1) and potential weathering rate P_0 in Eq. (4). Below-freezing conditions are not considered here.

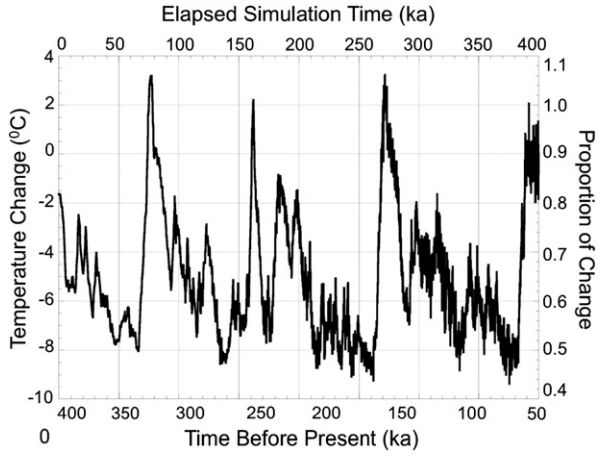


Figure 2. Temperature Reconstructions from the Vostok Ice Core Stable Isotope Data (Petit et al., 1999; downloaded from http://www.ncdc.noaa.gov/paleo/icecore/antarctica/vostok/vostok_isotope.html) and its corresponding effect on the simulated processes. We assumed a linear 5% decrease in weathering rate and runoff discharge for every 1 °C cooling.

Simulation settings

For simplicity of interpretation we use a synthetic hillslope with longitudinal profile (25 nodes, 16% topographic slope; Fig. 1a) and focus on the evolution of the grading of the soil surface. The hillslope used here is planar (Fig. 1a), so erosivity increases with increasing runoff discharge in the downslope direction. At the start of the simulations the profile layers are initialized with 100% bedrock overlain by a thin surface layer (0.5 cm thick) containing soil (initially spatially uniform with a median diameter (d_{50}) of 3.34 mm (Table 1)).

The simulations discussed here are for 400 ka with a 0.1-yr time step (a total of 4 million iterations). The landscape is divided into 4×4 m nodes with 20 vertical soil-profile layers (each 10 cm thick; Fig. 1b) plus a thin surface layer (0.5 cm thick). Soil particle-size distribution is represented by 23 size classes (Table 1).

Results and discussion

The evolution of surface soil grading (summarised by d_{50}) on the hillslope is as follows (Fig. 3). Initially the surface grading coarsens rapidly as the eroded material from the surface is refurbished by coarse material from the, as yet, unweathered underlying soil profile. This trend is reversed after 10 ka by a combination of low surface erosion (due to an absence of entrainable material, i.e. source-limited sediment transport) and the development of the underlying soil-profile by weathering. This stage of the evolution (resulting from model spin-up) takes about 70–90 ka and is approximately linear with time. The linearity of this initial phase indicates that it is relatively unaffected by the climatic fluctuations (Fig. 3a) and largely a function of model initialisation.

After the initial development stage (70–90 ka long) the evolution follows the longer-term climatic oscillations (Fig. 3) with the soil in dynamic equilibrium with, but slightly lagging, climate fluctuations. This temporal lagging of surface soil grading indicates that the soil–landscape response to climate fluctuations is not immediate; rather it requires a significant adjustment period even in response to relatively moderate climate changes. Following sharp climatic changes (i.e. the 10 ka transition from glacial maximum to peak interglacial conditions) surface soil grading requires a substantial adjustment period before returning to the dynamic equilibrium it exhibit under moderate climatic fluctuations. For example, the sharp warming at

Table 1
Soil-grading size classes and corresponding initial surface particle-size distribution (modified from Willgoose and Riley, 1998).

Size-class diameter (mm)	Material retained (%)
0	0.35
0.016	0.35
0.032	0.35
0.0475	0.35
0.063	0.75
0.0795	0.75
0.096	0.75
0.111	0.375
0.118	0.375
0.125	0.575
0.156	0.575
0.187	1.15
0.25	10.2
0.5	4.8
0.75	4.8
1	6.25
1.5	6.25
2	8.2
3	8.2
4	10
6.75	10
9.5	24.6
19	0

https://doi.org/10.1016/j.yqres.2013.01.001 Published online by Cambridge University Press

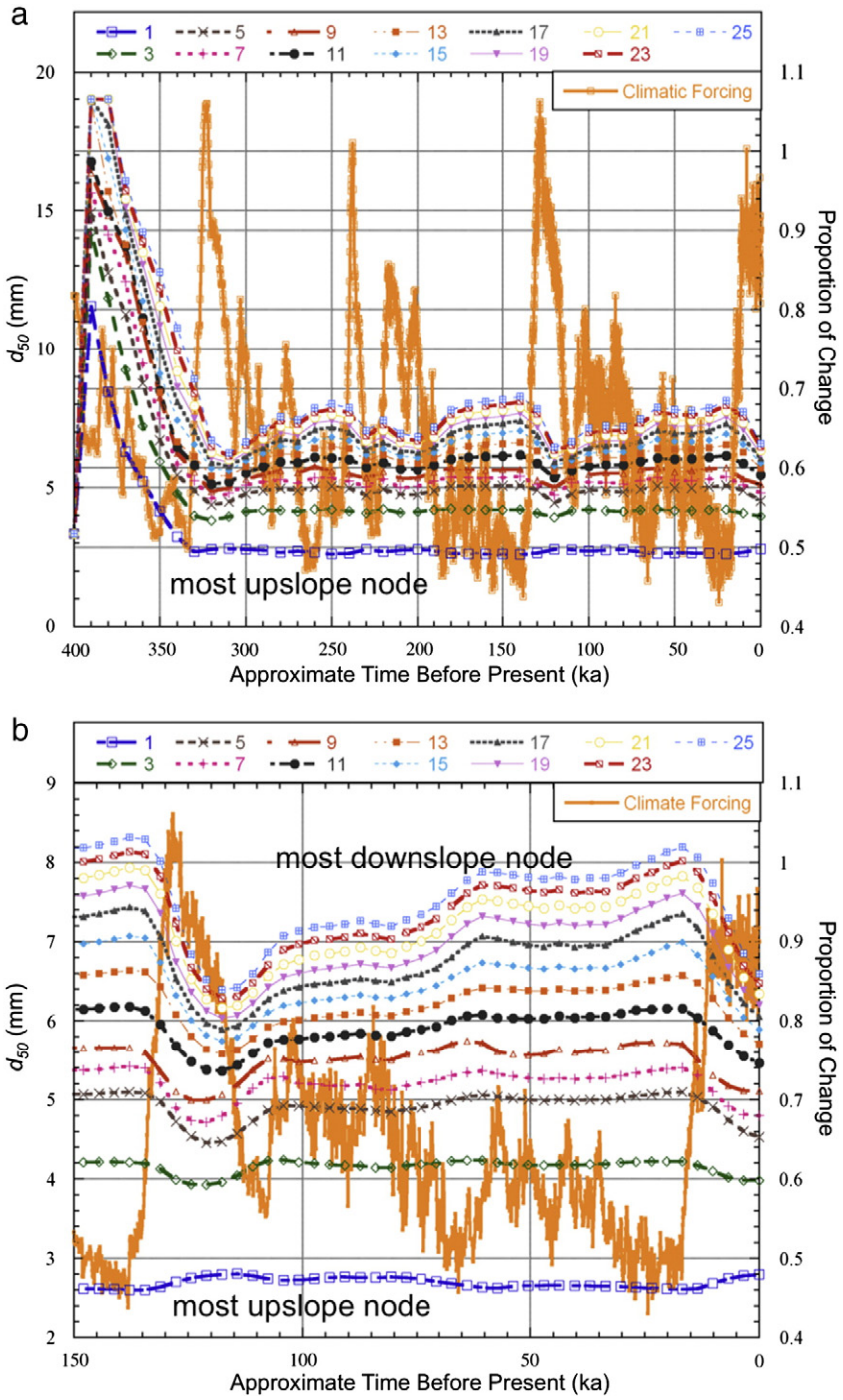


Figure 3. Surface soil-grading evolution (d_{50}- median diameter in mm; left axis) for every second node on the hillslope (nodes 1 and 25 are at the top and bottom of the hillslope respectively; Fig. 1a) and the climatic forcing (right axis). a: the whole 400 ka simulation. b: enlargement of the last 150 ka of the simulation.

the end of marine oxygen isotope stage (OIS)-6 (140 ka; left-hand side in Fig. 3b) triggers a rapid grain-size reduction (decreasing d_{50}) for most of the hillslope that continues for 10 ka after the climate cools. Surface fining only comes to an end when the climate starts to cool more rapidly (at ~120 ka), which suggests that the 10 ka adjustment lag would have been longer under continuously moderate cooling. This adjustment period also varies in space as the upper sections of the hillslope reach new equilibrium conditions approximately 5 ka quicker than the downslope nodes (Fig. 3b).

There is a consistent spatial trend in the response of surface soil grading to the climatic fluctuations: an increase in d_{50} fluctuations at the downslope direction i.e. soil grading is increasingly responsive to climate change at the downstream direction. Notably the topmost node (#1 in Fig. 3) has a cyclic response that is opposite to that of the downslope nodes, an increase in d_{50} with climatic warming (best seen in Fig. 3b). This happens because the relationship between weathering and erosion rates is spatially variable. Here we assume that on a planar hillslope runoff and erosion will increase in the downslope direction while the weathering rate remains constant. This means that changes in the interplay between weathering rate and runoff, induced by climate fluctuation, will be different depending on the location on the hillslope with weathering dominating at the top of the hillslope, and erosion more dominant at the bottom of the hillslope.

https://doi.org/10.1016/j.yqres.2013.01.001 Published online by Cambridge University Press

To further investigate these results a simple step-change climate scenario was simulated (Fig. 4). For the first half of the simulation (200 ka) climatic forcing was kept constant, at LGM climate, resulting in a time-constant equilibrium surface soil grading (Fig. 4). The climate then allowed to warm to peak interglacial conditions over 1 ka to simulate rapid climate change. The climate is then held constant at peak interglacial conditions for a further 199 ka, allowing the soil to reach a new equilibrium.

The differences in surface d_{50} before and after the sharp climatic shift (Fig. 4) range from a decrease of 2.23 mm at the bottom of the hillslope (node 25; a decrease of 26.9%) to an increase of 0.143 mm at the top of the hillslope (node 1; an increase of 5.5%). This means that the surface soil grading to the bottom of the hillslope became finer in response to climatic warming and the top of the hillslope became coarser. This is surprising as here we assume that runoff will increase in warmer climates promoting higher erosion rates resulting in coarser surfaces. The reason for this counterintuitive trend is variations in erosion regimes along the hillslope. The downslope nodes are under a source-limited erosion regime before the climate change due to a developed surface armor. The increase in runoff discharge had relatively little effect, as the limiting factor is entrainable sediment at the surface. However the increase in weathering rate led to a more-developed soil profile which in turn supplied finer sediment to the surface, resulting in lower surface d_{50}. The upslope-most node showed a cyclic response to climate change as it is under a transport-limited erosion regime and thus more affected by the increase in runoff discharge leading to surface coarsening.

Fig. 4 shows that it can take a considerable amount of time (tens of thousands of years) for a soil–landscape to reach new equilibrium conditions in response to a sharp climate change. The length of the adjustment period to the new climate decreases upslope, from more than 20 ka at the bottom of the hillslope to about 10 ka at the top (Fig. 4). These values are consistent with the simulation using the Vostok ice-core climate data (Fig. 3). The adjustment period was longer for nodes undergoing greater change in surface d_{50} in response to climate change. This shows that the soil–landscape adjustment rate in spatially variable. These results suggests that modern soil and landscape may still be adjusting to the LGM and that the strength of the LGM legacy within the landscape is highly spatially variable.

Overall the results show that soil–landscape evolution has a complex non-linear spatial and temporal response to climate change, even over this small and simple landscape and using a simplified model. For example, the change between the first and second equilibrium d_{50} in Fig. 4 varied non-linearly with distance downslope (Fig. 5). This implies that the spatio-temporal uniformity in which soil is typically described in Earth system modeling (Willgoose and Hancock, 2010) and analysis (e.g. carbon cycle) grossly underestimates their actual complexity.

Conclusions

This study explores a narrow set of soil–landscape interactions, the effect of mid and late Quaternary climate fluctuations on surface soil-grading spatiotemporal dynamics. It provides conceptual understandings of the potential mineralogical pedogenesis response to climatic forcing. The value of this study is that it sets the stage for more complex sensitivity analysis explorations such as soil–landscape-vegetation dynamics and landscape morphology response to climatic forcing.

The results demonstrate how the affect of external drivers on the rate of, and thus the dynamics between, soil–landscape processes triggers considerable changes in soil properties. Under moderately slow changes (relative to the soil response time) soil–landscape may reach new equilibrium conditions relatively in sync with the external driver (i.e. it will reach dynamic equilibrium). However, when the rate of the change exceeds the rate at which soil can adjust the soil–landscape evolution processes will lag the external driver and new equilibrium conditions may be reached long after the change occurred (up to 30 ka in this study). This suggests that many soil–landscapes around the world are still "recovering" from the LGM and should not be assumed to be in study-state. The legacy of the LGM on natural systems was documented in the literature mostly for large basins (Dosseto et al., 2008) where the impact of climate change is mainly through vegetation and land-use dynamics (Dosseto et al., 2010). The results here add the sediment production mechanism (i.e. soil

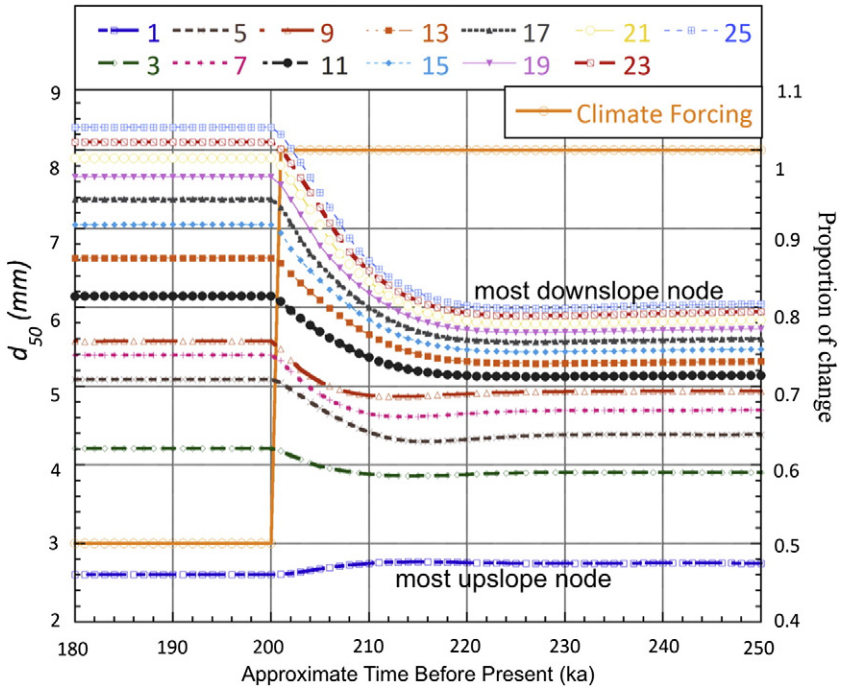


Figure 4. Surface soil-grading evolution (d_{50}- median diameter in mm; left axis) for every second node on the hillslope (nodes 1 and 25 are at the top and the bottom of the hillslope respectively; Fig. 1a) and the climatic forcing (right axis) using a one-step climate-change dataset.

https://doi.org/10.1016/j.yqres.2013.01.001 Published online by Cambridge University Press

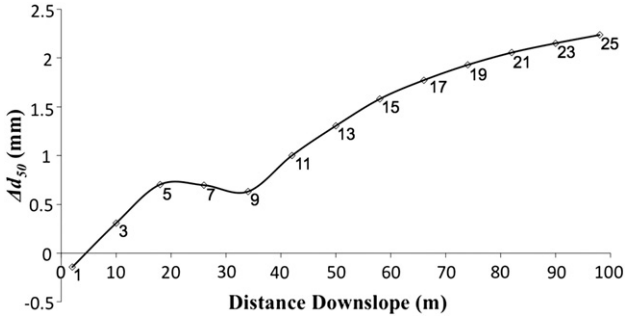


Figure 5. Changes in surface d_{50} between equilibrium values before and after climate change (Fig. 4) in each second node (numbers corresponds to Figs. 3 and 4) downslope. This is an example of the non-linearity of soil–landscape evolution response to climate fluctuations.

weathering and transport from the hillslopes) as a potentially significant source of temporal variability for the whole source-to-sink system.

Acknowledgments

GW was supported by an Australian Research Council Australian Professorial Fellowship. Part of the modelling and analysis was conducted using the Community Surface Dynamics Modeling System (CSDMS; University of Colorado Boulder) computing resources. We thank the anonymous reviewers for their constructive comments.

References

Birkeland, P.W., 1974. Soils and Geomorphology. Oxford University Press, New York (372 pp.).
Chadwick, O.A., Nettleton, W.D., Staidl, G.J., 1995. Soil polygenesis as a function of Quaternary climate change, northern Great Basin, USA. Geoderma 68 (1–2), 1–26.
Cohen, S., Willgoose, G., Hancock, G., 2009. The mARM spatially distributed soil evolution model: autationally efficient modeling framework and analysis of hillslope soil surface organization. Journal of Geophysical Research - Earth Surface 114, 15.
Cohen, S., Willgoose, G., Hancock, G., 2010. The mARM3D spatially distributed soil evolution model: three–dimensional model framework and analysis of hillslope and landform responses. Journal of Geophysical Research - Earth Surface 115, 16.
Cornu, S., Montagne, D., Vasconcelos, P.M., 2009. Dating constituent formation in soils to determine rates of soil processes: a review. Geoderma 153, 293–303.
Coventry, R.J., 1976. Abandoned shorelines and the Late Quaternary history of Lake George, New South Wales. Journal of the Geological Society of Australia 23, 249–273.
Cox, P.M., Betts, R.A., Jones, C.D., Spall, S.A., Totterdell, I.J., 2000. Acceleration of global warming due to carbon-cycle feedbacks in a coupled climate model. Nature 408, 184–187.
Dosseto, A., Bourdon, B., Turner, S., 2008. Uranium-series isotopes in river materials: Insights into the timescales of erosion and sediment transport. Earth and Planetary Science Letters 265, 1–17.
Dosseto, A., Hesse, P.P., Maher, K., Fryirs, K., Turner, S., 2010. Climatic and vegetation control on sediment dynamics during the last glacial cycle. Geology 38, 395–398.
Gibbs, M.T., Kump, L.R., 1994. Global chemical erosion during the last glacial maximum and the present: sensitivity to changes in lithology and hydrology. Paleoceanography 9 (4), 529–543.
Gislason, S.R., Oelkers, E.H., Eiriksdottir, E.S., Kardjilov, M.I., Gisladottir, G., Sigfusson, G., Snorrason, A., Elefsen, S., Hardardottir, J., Torssander, P., Oskarsson, N., 2009. Direct evidence of the feedback between climate and weathering. Earth and Planetary Science Letters 277, 213–222.
Heimsath, A.M., Dietrich, W.E., Nishiizumi, K., Finkel, R.C., 1997. The soil production function and landscape equilibrium. Nature 388, 358–361.
Heimsath, A.M., Chappel, J., Dietrich, W.E., Nishiizumi, K., Finkel, R.C., 2001. Late Quaternary erosion in southeastern Australia: a field example using cosmogenic nuclides. Quaternary International 83–85, 169–185.
Holmes, K.W., Roberts, D.A., Sweeney, S., Numata, I., Matricardi, E., Biggs, T., Batista, G., Chadwick, O.A., 2004. Soil databases and the problem of establishing regional biogeochemical trends. Global Change Biology 10, 796–814.
Jenny, H., 1941. Factors of Soil Formation; a System of Quantitative Pedology. McGraw–Hill.
Leeder, M.R., Harris, T., Kirkby, M.J., 1998. Sediment supply and climate change: implications for basin stratigraphy. Basin Research 10 (1), 7–18.
Minasny, B., McBratney, A.B., 2006. Mechanistic soil-landscape modelling as an approach to developing pedogenetic classifications. Geoderma 133, 138–149.
Murphy, B.W., 2007. The nature of soil. In: Charman, P., Murphy, B.W. (Eds.), Soils: Their Properties and Management. Oxford University Press, South Melbourne.
Pan, Y., McGuire, A.D., Kicklighter, D.W., Melillo, J.M., 1996. The importance of climate and soils for estimates of net primary production: a sensitivity analysis with the terrestrial ecosystem model. Global Change Biology 2 (1), 5–23.
Petit, J.R., et al., 1999. Climate and atmospheric history of the past 420,000 years from the Vostok ice core, Antarctica. Nature 399, 429–436.
Quinton, J.N., Govers, G., Van Oost, K., Bardgett, R.D., 2010. The impact of agricultural soil erosion on biogeochemical cycling. Nature Geoscience 3, 311–314.
Schenk, H.J., Jackson, R.B., 2002. Rooting depth, lateral root spreads and below ground/above-ground allometries of plants in water limited ecosystems. Journal of Ecology 90 (3), 480–494.
Sharmeen, S., Willgoose, G.R., 2006. The interaction between armouring and particle weathering for eroding landscapes. Earth Surface Processes and Landforms 31, 1195–1210.
Sitch, S., et al., 2003. Evaluation of ecosystem dynamics, plant geography and terrestrial carbon cycling in the LPJ dynamic global vegetation model. Global Change Biology 9, 161–185.
Sommer, M., Gerke, H.H., Deumlich, D., 2008. Modelling soil landscape genesis — a "time split" approach for hummocky agricultural landscapes. Geoderma 145, 480–493.
Temme, A.J.A.M., Veldkamp, A., 2009. Multi-process Late Quaternary landscape evolution modelling reveals lags in climate response over small spatial scales. Earth Surface Processes and Landforms 34 (4), 573–589.
Wells, T., Binning, P., Willgoose, G., Hancock, G., 2006. Laboratory simulation of the salt weathering of schist: I. Weathering of schist blocks in a seasonally wet tropical environment. Earth Surface Processes and Landforms 31, 339–354.
Wells, T., Willgoose, G.R., Hancock, G.R., 2008. Modeling weathering pathways and processes of the fragmentation of salt weathered quartz-chlorite schist. Journal of Geophysical Research-Earth Surface 113, 12.
West, A.J., Galy, A., Bickle, M.J., 2005. Tectonic and climatic controls on silicate weathering. Earth and Planetary Science Letters 235, 211–228.
White, A.F., Blum, A.E., 1995. Effects of climate on chemical weathering in watersheds. Geochimica et Cosmochimica Acta 59, 1729–1747.
Willgoose, G.R., Hancock, G.R., 2010. Applications of long-term erosion and landscape evolution models. In: Morgan, R.P.C., Nearing, M.A. (Eds.), Handbook of Erosion Modelling. Wiley-Blackwell, Oxford.
Willgoose, G.R., Riley, S., 1998. The long-term stability of engineered landforms of the Ranger Uranium Mine, Northern Territory, Australia application of a catchment evolution model. Earth Surface Processes and Landforms 23, 237–259.
Zembo, I., Trombino, L., Bersezio, R., Felletti, F., Dapiaggi, M., 2012. Climatic and Tectonic Controls On Pedogenesis and Landscape Evolution In A Quaternary Intramontane Basin (Val D'agri Basin, Southern Apennines, Italy). Journal of Sedimentary Research 82, 283–309.
Zhang, P., Molnar, P., Downs, W.R., 2001. Increased sedimentation rates and grain sizes 2–4 Myr ago due to the influence of climate change on erosion rates. Nature 410, 891–897.

https://doi.org/10.1016/j.yqres.2013.01.001 Published online by Cambridge University Press